Iranian Journal of Electrical and Electronic Engineering 01 (2019) 14–28
Special Issue on Power Engineering

IUST Iran University of Science and Technology

Iranian Journal of Electrical and Electronic Engineering

Journal Homepage: ijeee.iust.ac.ir

A New Approach for Transformer Interturn Faults Detection Using Vibration Frequency Analysis

S. Hajiaghasi*(C.A.), K. Abbaszadeh** and A. Salemnia*

Abstract: Interturn fault detection is a challenging issue in power transformer protection. In this paper, interturn faults of distribution transformer are studied and a new online detection method based on vibration analysis is proposed. Transformer electromagnetic forces are analyzed by time stepping finite element (TSFE) modeling of interturn fault. Since the vibration associated with inter-turn faults is caused by electromagnetic forces, axial and radial electromagnetic forces for various interturn faults are studied. Transformer winding vibration under interturn faults is studied through an equivalent mathematical model combined with electromagnetic force analysis. The results show that it is feasible to predict the interturn winding faults of transformer windings with the transformer vibration analysis method. Simulation and experimentation studies are carried out on 20/0.4 kV, 50 kVA distribution transformer. The results confirm the effectiveness of the proposed method.

Keywords: Transformer, Vibration, Interturn Fault, Electromagnetic Force.

1 Introduction

DEMANDS growth for safe and reliable electrical energy supply is important factor from power suppliers and consumers point of view [1]. Transformer faults can be categorized into internal and external types. Statistics shows that 70–80% of the power transformers damages arise from internal faults. Among the internal faults, winding faults (interturn and layer to layer, phase–to–ground and phase to phase faults) are the most important internal faults in transformers. Detection of winding interturn fault, particularly at low current is critical. The interturn faults have large impact on the transformer lifetime [2]. Initial detection of the interturn fault in power transformers is so important due to high cost and a lot of time to repair. This is more important particularly for transformers nearing the end of their lifetime in which fault is more expected. The percent of various faults in transformers are shown in Fig. 1 [3]. It should be noted that about 30% of failures are due to the winding faults. As initial winding short circuit occurs, the location of short circuit is overheated. Overheating causes winding insulator deterioration and fault extension [4]. Early influence of these faults is very little on transformer primary and secondary line currents so there is not the possibility of using fuses or differential relays for detection of these faults. There have been many investigations on internal short circuit faults modeling in power transformers throughout the literature [4-8]. It can be concluded that finite element method (FEM) is a powerful and precise numerical technique for transformer interturn fault modeling [9].

Various methods are used for transformer interturn fault detection [10]. A summary of different methods used for interturn fault detection is given in Table 1.

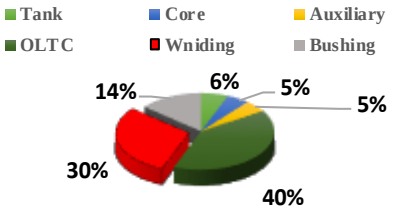

Fig. 1 The block diagram of the considered hybrid micro grid.

Iranian Journal of Electrical and Electronic Engineering, 2019.
Paper first received 17 February 2018 and accepted 11 June 2018.
* The authors are with the Department of Electrical Engineering, Shahid Beheshti University, Tehran, Iran.
E-mails: s_hajiaghasi@sbu.ac.ir and a_salemnia@sbu.ac.ir.
** The author is with the Department of Electrical Engineering, Khaje Nasir Toosi University of Technology, Tehran, Iran.
E-mail: abbaszadeh@kntu.ac.ir.
Corresponding Author: S. Hajiaghasi.

Table 1 Summary of interturn faults detection methods.

Detection Method	Advantage	Limitation	Online Detection	Literature
DGA	- Detection of any abnormality at incipient level.	- Expensive - Has some ambiguities in its analysis - Not useful for oil less transformer	✓	[11-13]
FRA	- Capacitive effect can be detected at high frequency.	- This method needs previous data on the transformer. - This method needs Complicated tool for detection.	✓	[14-16]
Negative Sequence	- The signal for fault detection is available.	- Cannot be used for unbalance load -This method is complicated	✓	[17, 18]
PD	-Well established method in power utilities.	- This method Impressive from tank and winding.	✓	[19, 20]
Flux Based Method	- Method accurate is good. - Method can detect fault location exactly.	- Change in transformer structure - Models developed for verification purpose. - Requires the details of the transformer structure and sensors.	✓	[21-24]
Voltage and Current Measurement	- Models developed for verification purpose.	- For unbalance load cannot be used.	✓	[25-27]
Differential Protection	- Classical and robust method. - On line monitoring is possible.	- Unable to detect interterm fault at inception level. - Depends largely on the precision of current transformer (CT). - Sensitivity of this technique to winding insulation breakdown. - Sensitive to the structure of transform.	✓	[28-30]
Intelligent Approach	Detect minute faults, robust for missing data.	- More training data required. - Problem of local minima, memory and computations.	✓	[31-34]
Vibration Analysis	- This method can detect mechanical and electrical fault.	- Vibration model is complicated. - Sensor must mounted on winding.	✓	[35, 36]

Interturn faults must be detected as soon as possible, so between techniques reviewed in Table1, online-based methods are more attractive. Although most methods have online capability detection but the complexity and precision of the method should also be considered. Vibration-based methods have good feature for interturn faults detection. Although most researches have studied the transformer vibration, there have been little in-depth researches on winding vibration and none of them have investigated vibration analysis for interturn faults. The study of winding vibration can be divided into two steps. The first step is to obtain the distributed electromagnetic forces within the winding. Next, the winding vibration is calculated through an equivalent mathematical model [35]. Electromagnetic forces usually are calculated for short circuit condition. Because of transformer complicate structure, FEM based methods successfully are used for transformer electromagnetic force calculation [37-39]. An accurate understanding of the vibration characteristics of transformers is necessary for detecting electrical and mechanical faults in a transformer using vibration-based monitoring techniques. Some researchers have explored the inherent mechanical characteristics of windings [40-43]. Analysis of transformer electromagnetic vibration noise are presented in [44]. In [45], the transmission of vibration (from winding to tank) is examined experimentally in a 110 kV power transformer with and without cooling oil. Reference [46] describes a method for detecting faults in the tap selector by means of vibration measurements during tap changer operation, using envelope analysis based on Hilbert transform and Wavelet decomposition.

However, most of the existing research focuses on the winding vibration under normal conditions, winding deformation, mechanical faults and none of them investigate transformer vibration analysis under interturn faults. In this paper, transformer winding vibration under interturn fault are studied through an equivalent mathematical model combined with electromagnetic force analysis. Since the vibration associated with inter-turn faults is caused by electromagnetic forces, axial and radial electromagnetic forces for various interturn faults are studied. Experimental tests for simulation verification are done by a new method that uses ADXL330 sensor for vibration measurement. This paper is arranged as follows: first faulty transformer modeling is presented in Section 2. Then, faulty transformer analysis is presented in Section 3. Simulation and experimental results, are presented in Section 4 and Section 5 respectively. Finally, conclusions are given in Section 6.

2 Faulty Transformer Finite Element Modeling

A three-phase three-leg core-type transformer is modeled by the 2 dimension time stepping finite element method. Specifications of the proposed transformer are presented in Table 2. In transformer modelling, the dimensions of the core is exactly similar to those of actual core of laboratory transformer. High voltage (HV) and low voltage (LV) windings are also modelled with actual dimensions. The magnetization characteristic of the core material provided by the manufacturer is used.

Because of different magnitude of flux density in each part of the core, to calculate the exact electromagnetic force under various interturn short circuit, HV windings is divided into 20 sections and LV windings is divided into 90 sections; then axial and radial electromagnetic force in each section of windings is calculated. Using the Maxwell's equations, the computation of the magnetic field in the geometry of the transformer with the Coulomb gauge can be shown as (1)

$$\nabla\times\left(\frac{1}{\mu}\nabla\times A\right)+\sigma\left(\frac{\partial A}{\partial t}+\nabla V\right)=J_s \qquad (1)$$
$$\nabla.A=0$$

where A is the vector of magnetic potential, J_s is current density, μ is the magnetic permeability, σ is the electric conductivity and $\nabla.A = 0$ is the Coulomb gauge. Generally, transformer transient analysis is divided into two parts: formulation of electromagnetic FE and connection of external circuit.

In FEM, electric and magnetic circuit are coupled and matrix equations are solved at each step time to model dynamic behavior of the transformer. When a turn to turn fault on the transformer windings occurs, the distribution of the electromagnetic field inside the transformer and the terminal values in the circuit domain alter. Maxwell equations can describe the behavior of the transformer regardless of the health or faulty conditions.

The principle used to model various internal winding fault is to divide the winding which across it the interturn fault occurs in two parts: the faulty part and the rest coils in the circuit.

Transformer geometry and coils to model the interturn fault is shown in Fig. 2.

To create the interturn fault by FEM, modification of the geometry domain and circuit domain is necessary. Modelling of internal fault on HV winding is shown in Fig. 2(c). As illustrated in Fig. 2(c), limiting fault resistance (R_f) is utilized to initiate the fault on the winding. In fact, the fault resistance models the resistive part of the dielectric material in the dielectric equivalent parallel circuit model of the shorted turns. However, the fault severity depends on fault impedance and the number of shorted turns. Therefore, with the developed FEM of the transformer, internal winding faults can be simulated at different part of LV and HV windings with different levels of severity.

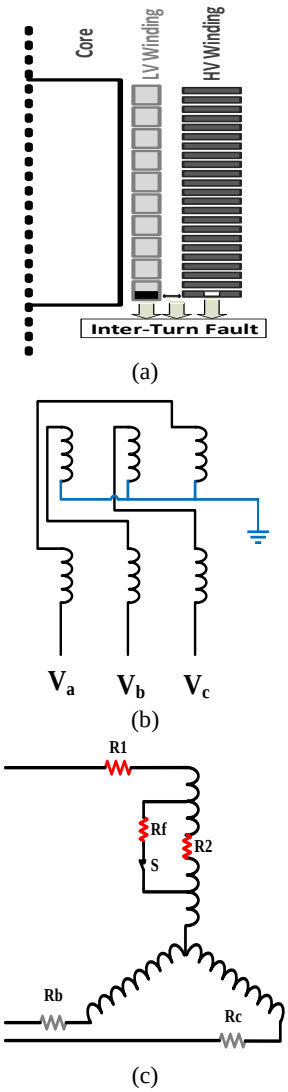

Fig. 2 Transformer internal fault modelling, a) Geometry domain, b) LV circuit domain and c) HV circuit domain.

Table 2 Transformer specifications.

Quantity	Value	Unit
Primary voltage	20	kV
Secondary voltage	0.4	kV
Rated power	50	kVA
No.of primary winding turns	4155	turn
Primary winding resistance /phase	100	Ω
No.of secondary winding turns	96	turn
Secondary winding resistance /phase	0.0089	Ω
Width of window	292	mm
Height of HV winding	225	mm
Height of LV winding	287	mm
LV radius	61.5	mm
HV radius	83.5	mm
Primary and secondary connection	Y/Z(zigzag)	
Cooling Method	ONAN	
Voltage regulation	4%	

3 Faulty Transformer Analysis

3.1 Leakage Flux Analysis

When transformer is working in stable operation, the flux density of iron heart and current in the windings are close to the rating. But when an interturn short circuit happens, the circulation current in faulty winding will be larger than the rated current. The transient magnetic flux, that includes the linkage and leakage flux, depends on the magnetization characteristic of core [47]. Especially, when interturn short-circuit occurs, the leakage flux density due to short-circuit current is increased enormously to several times the leakage flux density in the steady state operation. The leakage flux consists of radial and axial directions. To calculate the electromagnetic forces, first magnetic flux density should be yielded. This purpose will be obtained by solving electromagnetic potential vector equations as (2).

$$\nabla^2 A = \begin{cases} \mu_0 J & n \text{ windings} \\ 0 & \text{otherwise} \end{cases} \tag{2}$$

After calculation of electromagnetic potential, the components of leakage flux are expressed using vector potential as (3).

$$B = \nabla \times A = \vec{i}B_x + \vec{j}B_y \tag{3}$$

where, B_x and B_y, are directional components of leakage flux density [T], respectively. J is the current density, μ_0 is the air permeability. A is magnetic vector potential.

To transformer flux density analysis under normal and faulty conditions, the flux density of transformer for normal condition and faulty condition is given in Fig. 3. In Fig. 3(a) which shows transformer healthy state, magnetic flux lines pass vertically through the space between windings without any distortions so that if horizontal line passing through the middle of the transformer is assumed as reference axial, flux lines are totally symmetric with respect to this line. In Fig. 3(b), asymmetry in the distribution of magnetic flux lines under interturn fault is due to the increment of leakage flux and its radial component in the environment of linkage coils.

For transformer healthy state, leakage flux has a very small share of the total linkage flux and flux lines flow axially by passing through space between windings. Faraday rule states that induced electromotive force in a coil is proportional to the electromagnetic flux variation in the coil, so that for constant frequencies, the amount of electromagnetic flux entering the coil depends on the induced electromotive force in the coil terminals. Thus as the assumed coil is shorted, coil voltage decreases and circulating current created in coil, confines flux entering the coil. According to lens rule, circulating current in linkage coils is in the direction that resists its creating agent (input electromotive force). As a survey with ideal state, when a coli of complete conductivity is shorted through zero fault resistance, coil terminals voltage would be zero, therefore there is no flow of flux in the coil. It is evident as the coil conductivity and fault resistance decrease, more electromotive flux lines pass through the assumed coil and vice versa. Any way the limitation of electromagnetic flux entering into linkage coil causes more focus of linkage flux in linkage coils environment and symmetric distribution distortion of transformer magnetic flux .This is the cause for variation of search coils induced voltage in faulty state.

The electromagnetic force acting on the transformer winding is caused due to short-circuit current and leakage flux density. Magnetic flux density are decomposed into their radial and axial components. The electromagnetic forces may also be composed into their radial and axial components as (4).

$$F = I(-\vec{i}B_y + \vec{j}B_x) = \vec{i}F_x + \vec{j}F_y \tag{4}$$

where I is the winding section current, F_x is radial component of force and F_y is axial component of force. According to (4), radial force depends on the axial component of the magnetic flux density, whereas the axial forces depend on the radial component of the magnetic flux density [48].

3.2 Vibration Analysis

Vibration analysis has two goals: 1) Investigating interturn faults effects on transformer vibration, 2) experimental validation of electromagnetic forces

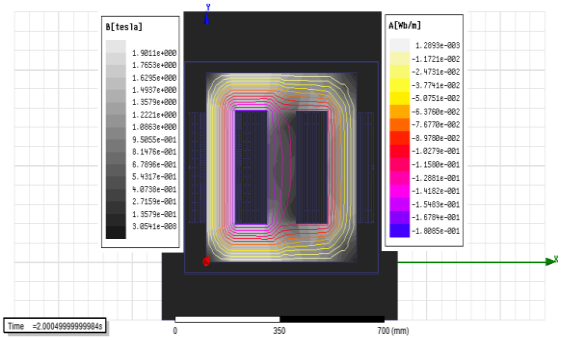

(a)

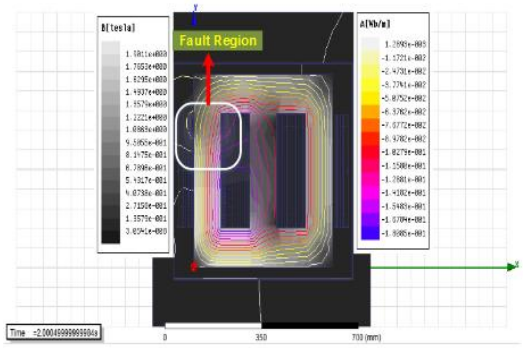

(b)

Fig. 3 Flux density and flux line, a) Healthy condition and b) Fault condition.

presented in the next section. Vibrations in the transformer are generated by the different forces appearing in the windings and core. The winding vibration is due to the electromagnetic forces caused by the interaction between the current circulating by a winding and the leakage flux. Referring to (4) forces are proportional to the current squared and have components in axial and radial directions. Since vibration depends on current squared, and considering that current is almost sinusoidal (50 Hz in this study), main harmonic of winding vibration is 100 Hz. The core vibration is caused by magnetostriction and magnetic forces. According to motion equations of mass, axial vibration model of the windings is built that is shown in Fig. 4.

Motion equations of mass elements can be written as (5).

$$\begin{cases} m_1\dfrac{d^2z_1}{dt^2}+c_1\dfrac{dz_1}{dt}+k_Bz_1+k_1(z_1-z_2)=F_1+m_1g \\ m_2\dfrac{d^2z_2}{dt^2}+c_2\dfrac{dz_2}{dt}+k_1(z_1-z_2)+k_2(z_2-z_3)=F_2+m_2g \\ m_n\dfrac{d^2z_n}{dt^2}+c_n\dfrac{dz_n}{dt}+k_{n-1}(z_{n-1}-z_n)+k_n(z_n-z_{n+1})=F_n+m_ng \\ m_N\dfrac{d^2z_N}{dt^2}+c_n\dfrac{dz_n}{dt}+k_{N-1}(z_{N-1}-z_N)+k_Hz_N=F_N+m_Ng \end{cases} \quad (5)$$

where m_n is mass of element n, k_n elastic coefficient of spacer block between disk n and disk n+1, k_B and k_H elastic coefficient of spacer block at winding ends, z_n is displacement of element n, c_n is friction coefficient, $m_n.d^2z_n/dt^2$ is inertial force of element n, $c_n.dz_n/dt$ is friction force of element n, $k_n(z_n - z_{n+1})$ is elastic force, F_n is electromagnetic force applied to element n, m_ng is weight of element n. Eq. (5) can be represented as (6).

$$[M]\frac{d^2\{z\}}{dt^2}+[C]\frac{d\{z\}}{dt}+[K]\{z\}=\{F\}+\{m\}g \quad (6)$$

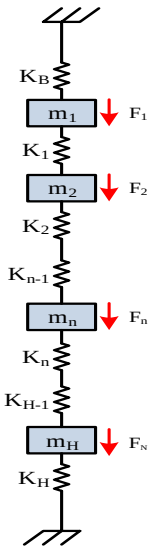

Fig. 4 Axial vibration model of transformer windings.

where

$$\{z\}=\begin{bmatrix} z_1 \\ z_2 \\ \vdots \\ z_N \end{bmatrix} \quad \{F\}=\begin{bmatrix} F_1 \\ F_2 \\ \vdots \\ F_N \end{bmatrix} \quad \{m\}=\begin{bmatrix} m_1 \\ m_2 \\ \vdots \\ m_N \end{bmatrix}$$

$$\{M\}=\begin{bmatrix} m_1 & & & 0 \\ & m_2 & & \\ & & \ddots & \\ 0 & & & m_N \end{bmatrix} \quad \{C\}=\begin{bmatrix} c_1 & & & 0 \\ & c_2 & & \\ & & \ddots & \\ 0 & & & c_N \end{bmatrix} \quad (7)$$

$$\{M\}=\begin{bmatrix} k_B+k_1 & -k_1 & & & & 0 \\ -k_1 & k_1+k_2 & -k_2 & & & \\ & -k_2 & k_1+k_2 & -k_3 & & \\ & & & \ddots & & \\ & & & -k_{N-2} & -k_{N-2}+k_{N-1} & k_{N-1} \\ 0 & & & & -k_{N-1} & k_{N-1}+k_H \end{bmatrix}$$

4 Simulation Result

First, transformer healthy state is simulated. Fig. 5 shows transformer HV current. It is known that inrush current is created at the start-up time due to core nonlinearity nature that is damped after a small time and the current reaches steady state amount. Transformer steady state LV current is shown in Fig. 6. Then simulations are carried out for a 3% (3% of total winding) turn fault in the LV winding firs layer with 5mΩ fault resistance. Fig. 7 shows HV currents. It should be noted that for the faults occurred in LV winding, only HV faulty phase and line current increase. Circulating current passing through shorted circuit windings are brought in Fig. 8. It is obvious that its amplitude in the shorted circuit winding is determined according to fault severity. Circulating current exists only in shorted circuit windings and the other parts current does not change and only depends on load and input voltage.

After modelling the faults of transformer in FEM, electromagnetic forces for various interturn faults are calculated. The result of radial forces in LV winding is shown in Fig. 9(a) for a 5% turn fault in phase A and on top of LV winding (fault resistance is 5 mΩ). In this state the fault is created in inner part of LV winding .The radial forces are negative if it flows to the tank and it will be positive if it flows to the core. It can be seen that radial forces compress LV winding to core side.The amount of radial forces around the fault location is bigger than other part of LV winding. This force may cause vibration of winding in the fault location. Fig. 9(b) shows axial forces in LV winding. It can be concluded that axial forces compress LV winding in Y-axis direction in fault location. Radial forces in HV winding are shown in Fig. 9(c). It shows that radial forces on the HV winding are exerted in the tank side direction. Amount of axial force in HV winding is small.

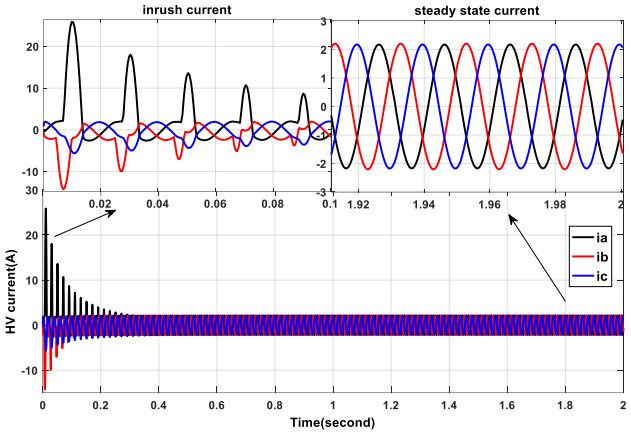

Fig. 5 HV currents from start-up to steady state.

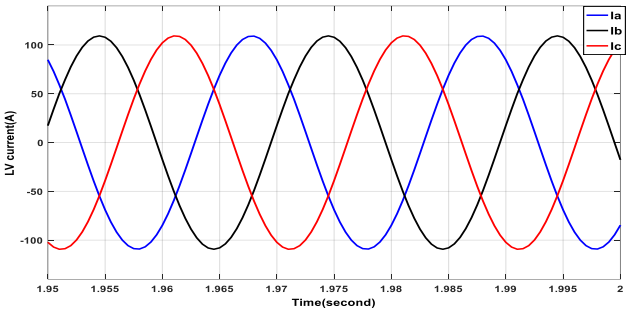

Fig. 6 LV currents.

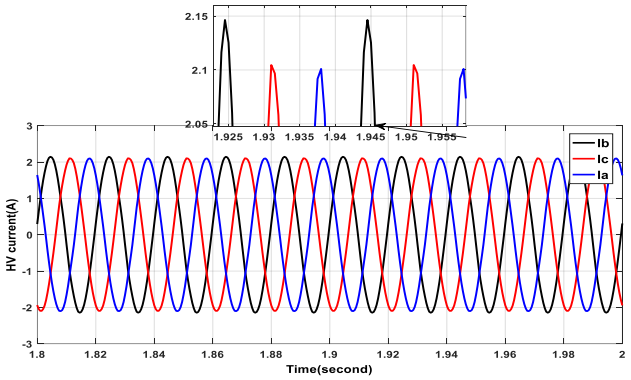

Fig. 7 HV currents under interturn fault.

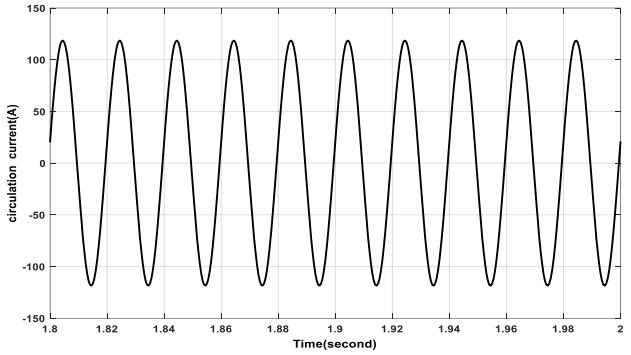

Fig. 8 Circulating current (fault current) in faulty windings.

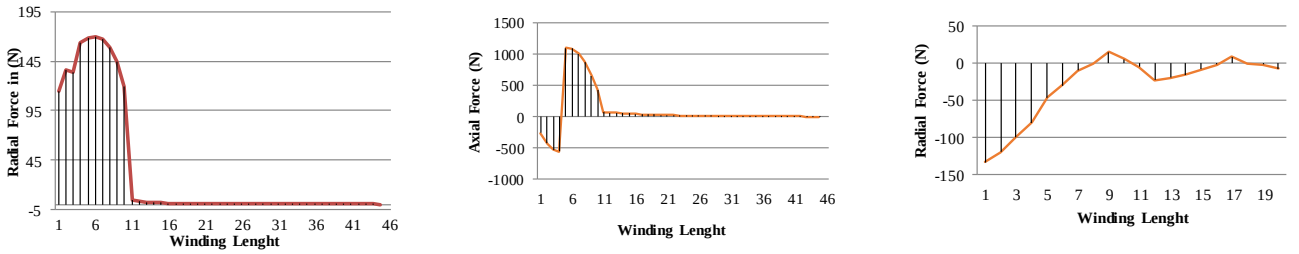

(a) (b) (c)

Fig. 9 Electromagnetic forces for 5% turn fault in phase A, a) Radial forces in LV winding, b) Axial forces in LV winding and c) Radial forces in HV winding.

4.1 Fault Location Effect

In this section the influence of location of interturn short circuit fault on electromagnetic force is investigated. For a constant fault severity (fault resistance is constant) in LV winding, the axial and radial electromagnetic forces for 3 different fault locations are calculated. Radial and axial forces in LV winding in these cases are shown in Fig. 10(a) and Fig. 10(b), respectively. These Figures represent when an interturn short circuit occurs, a high axial force compresses the fault location. For example, when fault occurs on the top of the winding, the upper parts of winding (that is shorted) are compressed. From Fig. 10(c) it can be seen that when fault occurs in the middle of winding, the forces are bigger than the other cases, this phenomenon occurs because the flux density in these locations of transformer is larger than other locations.

The results of radial forces for various interturn faults are shown in Table 3. To model HV to LV winding fault, the upper part of the high voltage coil is connected to the upper part of the low voltage coil. The fault resistance is considered 10 Ω in this case. From the results, it can be concluded that the faults between HV and LV windings are very dangerous. These types of faults are more dangerous than three short circuit faults, because enormous force is applied just to the fault location. The magnitudes of forces under these types of short circuit faults are very high that can lead to complete destruction of winding. This can be considered in the design of the transformer. Radial forces under

various interturn faults are shown in Table 4. It can be seen that magnitude of forces near fault location are larger than other locations.

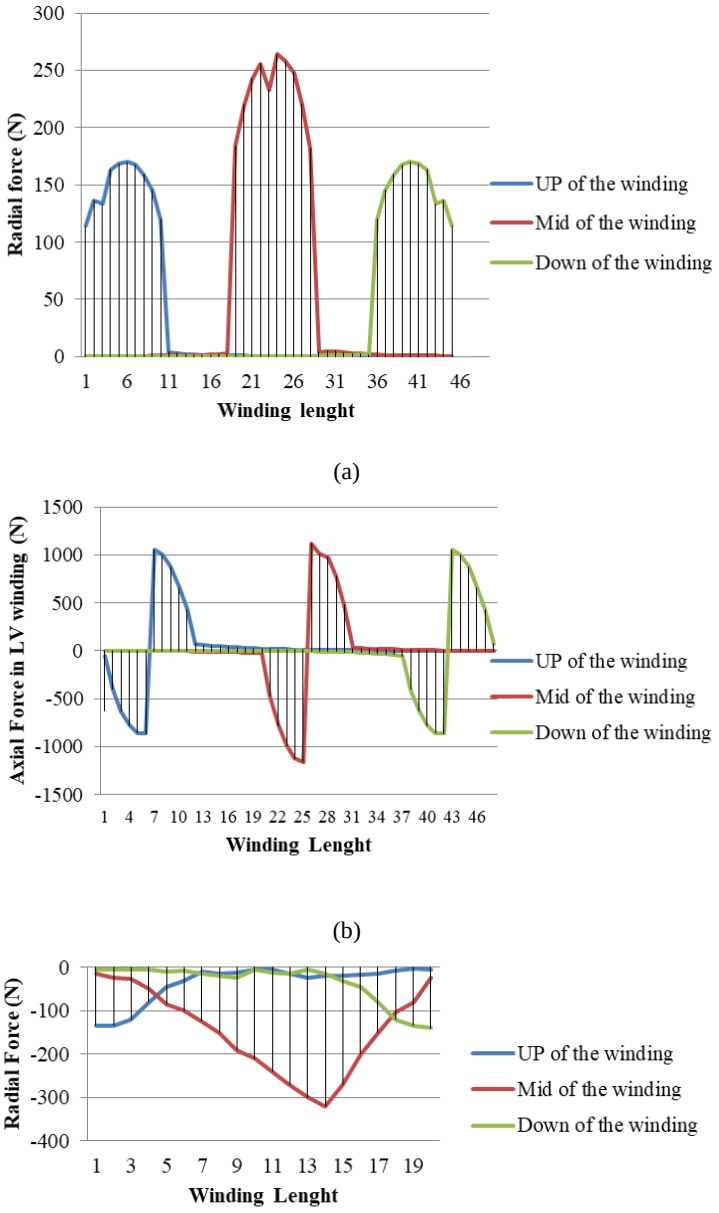

Fig. 10 Descriptive model of the proposed adaptive RL-PID controller.

Table 3 Radial force in LV and HV winding for various interturn fault types.

Interturn Fault Types / Height of Winding		1	2	3	4	5	6	7	8	9	10
5% the top of the LV winding	Force in LV (N)	143.49	118.7	2	1	0.6	0.52	0.49	0.47	0.32	0.28
	Force in HV(N)	-127	-90	-38	-5	10	-14.1	-18	-5	4.5	-4.8
5% the top of the HV winding	Force in LV(N)	-70.8	-226.9	-6.2	0	0	0	0	0	0	0
	Force in HV(N)	194.6	-55	26	18.4	10.64	5.7	-0.78	-0.53	-0.47	2.2
HV to LV interturn fault	Force in LV(kN)	67.8	164.42	228.4	253.4	261	258	240	200	140.2	56.5
	Force in HV(kN)	-1010	-1008	-1136	-931	-932	-1173	-931	-914	-887	-1.025

Table 4 Axial force in LV and HV winding for various interturn fault types.

Interturn Fault Types / Height of Winding		1	2	3	4	5	6	7	8	9	10
5% the top of the LV winding	Force in LV (N)	451	1018.1	305.7	48.5	28.3	13.5	6.9	1.7	-0.1	-2
	Force in HV(N)	-77.3	-182	-123.6	-54.2	-42	-30	-19.4	-11.4	-3.3	7.8
5% the top of the HV winding	Force in LV(N)	4.5	-37.2	6.3	0	0	0	0	0	0	0
	Force in HV(N)	210	3.7	-39.5	-22.4	-16.5	-10	-7.4	-4.4	-1.6	3
HV to LV interturn fault	Force in LV(kN)	-258.8	-27.47	32.76	19.28	5.6	-4.8	-20.1	-34.2	18.6	240
	Force in HV(kN)	-562.6	-231	-129.4	-37.9	-11.5	21.94	39.95	76.9	138	582.9

(a) (b)

Fig. 11 Faulty transformer and measurement system.

(a) (b) (c)

Fig. 12 Faulty transformer and measurement system.

5 Experimental Validation

5.1 Model Validation

A 50 kVA transformer is used to validate the simulation results. The parameters of the transformer is presented in Table 2. First transformer is disassembled and interturn faults are created in windings. To test different faults, windings come out from different locations of coils. Fig. 11 shows the transformer LV winding. For modelling various faults severity, various amounts of resistant are used in laboratory test. The results of tests were recorded through a 4-channel data acquisition system, with sampling time of 4×10^{-5} s. To measure the force, ADXL330 sensor is used. The ADXL330 is a small, thin, low power, complete three axis accelerometer with signal conditioned voltage outputs, all on a single monolithic IC. The product measures acceleration with a minimum full-scale range of ±3 g. It can measure the static acceleration of gravity in tilt-sensing applications, as well as dynamic acceleration resulting from motion, shock, or vibration. This sensor measures vibration in 3 axes (X, Y, Z). Sensor output is analog voltage proportional to axis vibration. Fig. 12 shows the transformer, data recorders and sensor mounted on HV winding in phase A.

Before doing the experiments, a full-load test was performed on the transformer to verify that the modifications had not changed the transformers' normal operating characteristics. In each experimental test, before doing the measurements, the transformer was allowed to stabilize within some minutes before the fault to correspond with the failure-free operation, so-called normal state of the transformer. After each test, the condition of the transformer was assessed by visual inspection and also performing a full load test to ensure that the fault had not damaged the transformer or not

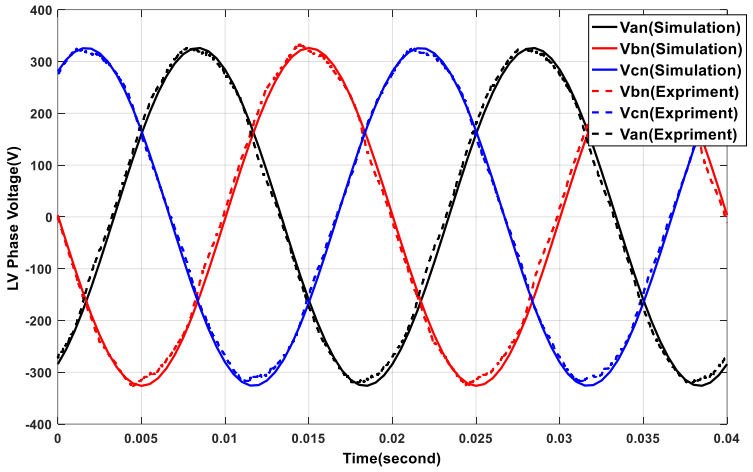

(a)

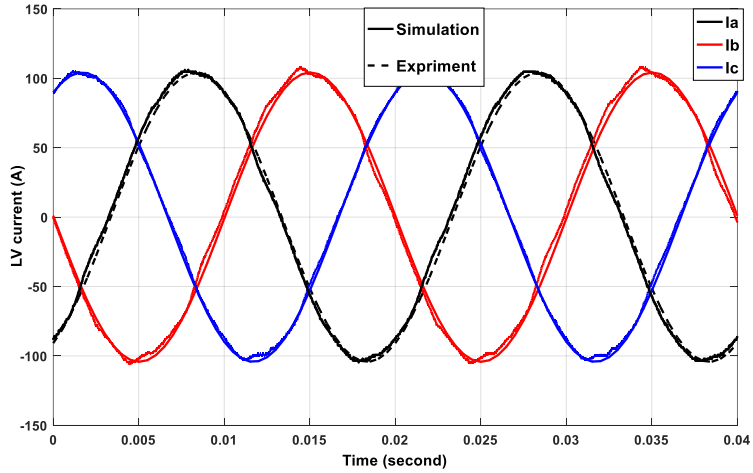

(b)

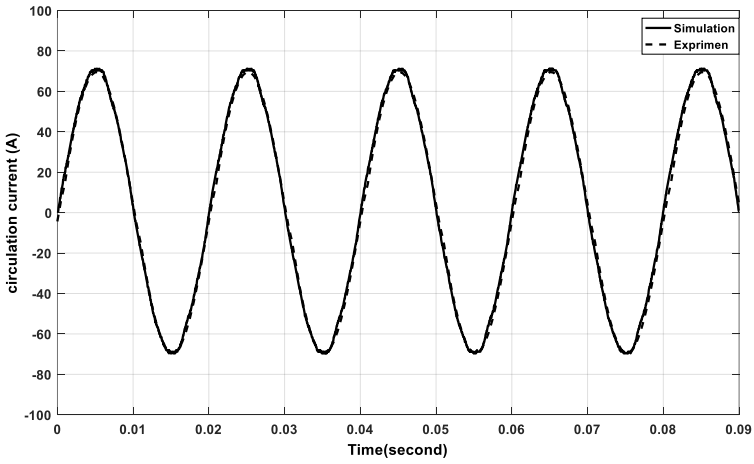

(c)

Fig. 13 Experimental test results, a) Comparison Three-phase LV phase voltages, b) Comparison Three-phase LV current, c) Comparison circulation current.

changed its characteristics. The comparison between simulated and experimental LV phase voltages for healthy condition are shown in Fig. 13(a). The results show the voltage signals are similar. LV currents in full load condition for resistive load are shown in Fig. 13(b), it is clear that experimental tests and simulation results confirm each other. Three-phase resistive load is 3.1 Ω which is connected to the LV side, in experimental case.

Fig. 13(c) shows circulating current for a 1% (1% of total winding) fault on top of the LV winding. Fault resistance in this case is 0.06 Ω (R_f = 0.06 Ω). From these figures, it is concluded that in faulty condition, experimental tests and simulation results are in agreement.

5.2 Vibration Analysis

When an interturn fault occurred in transformer winding, the current, leakage flux and electromagnetic force increase. When electromagnetic forces increase in axial and radial directions, the vibration of windings also increases. The amount of vibration increment depends on fault severity and sensor location. If fault severity increases, vibration amount increases too. For the same fault severity if fault occurs near the sensor location, vibration is larger than when fault occurs far from the sensor, but from various tests it is concluded that for different fault locations, in each phase vibration signal increases; that is because in transformers the HV and LV windings are tightly connected to each other and wrapped with insulation ribbons around the LV and HV windings that compresses winding tightly. Therefore to detect transformer fault by this method in each phase, one sensor must be used. To prove this claim, many tests have been carried out and 4 cases of these faults are brought in this paper. These faults are shown in Table 5. Y-axis frequency analysis for these cases are shown in Fig. 14. It can be seen that DC amount of vibration is increased in fault condition and for case 4, vibration is larger than case 2 with the same fault severity, it is because sensor is mounted close to the top of winding. Case 2 is a fault in the middle of the winding and its DC amount is larger than healthy state. Fig. 14 shows that at frequency 100Hz with increasing fault severity, the winding vibration increases based on Eq. (6).

Fig. 15 shows the vibration frequency spectrum along the X-axis. From these results it can be concluded that vibration frequency analysis can be used as an effective method for interturn fault detection. Considering vibration frequencies it can also be concluded for various faults severity and location, vibration frequencies spectrum changes which can be used to detect interturn fault location and severity by artificial intelligence methods. This method also can be used online more easily than other kinds of methods. Vibration analysis method which is descripted in this paper is a good method for transformer online monitoring.

Table 5 Test properties.

Number	Fault Severity	Fault Location	Phase
Case 1	Healthy	-	-
Case2	5% LV winding	Mid of winding	A Phase
Case3	3% LV winding	Down of winding	A Phase
Case4	5% LV winding	Top of winding	A Phase

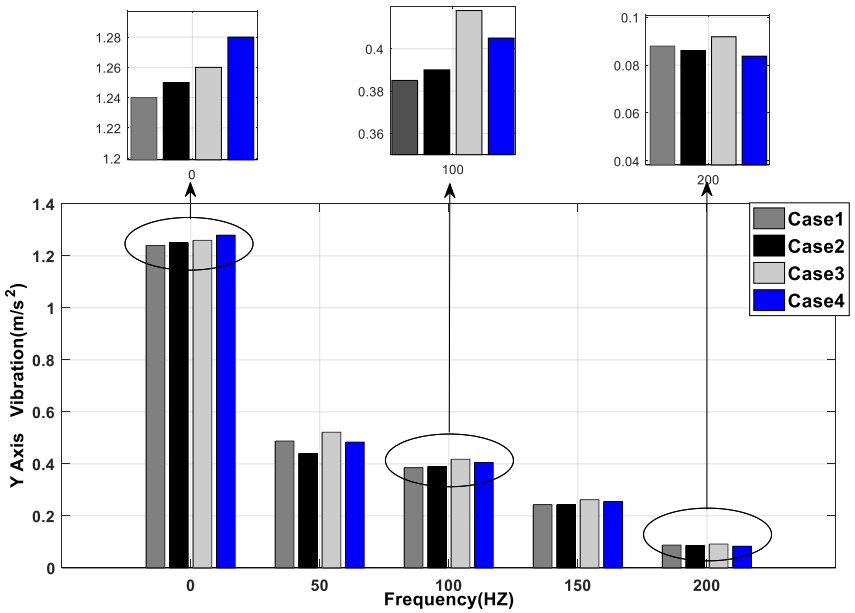

Fig. 14 FFT analysis of the Y axis vibration.

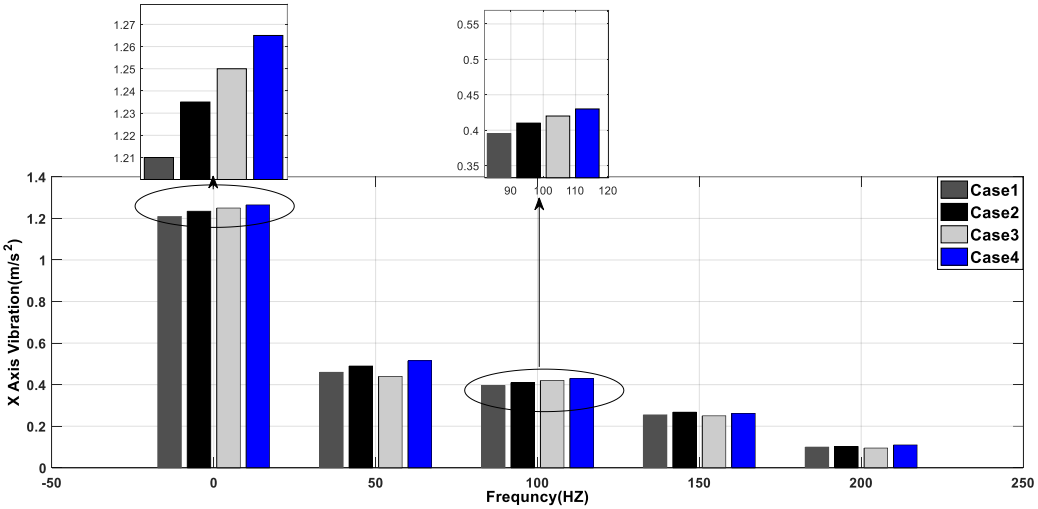

Fig. 15 FFT analysis of the X axis vibration.

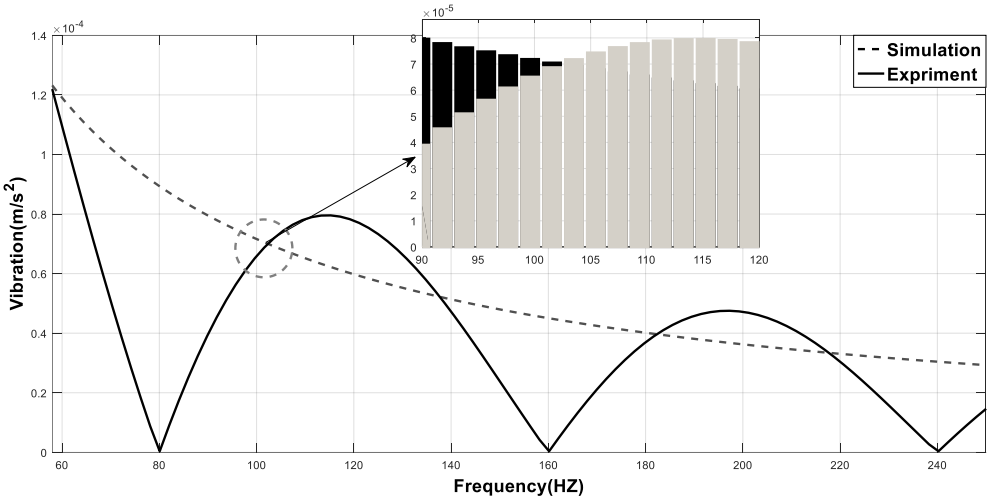

Fig. 16 FFT vibration analysis for experiment and simulation.

To calculate forces experimentally, a new method based on vibration analysis is used. First, transformer is modelled with a mass-spring equations that is described in Section 3.2. In experimental test, a 1% fault is created between LV turns in external LV coil. In transformer, various sources of vibrations exist and these vibrations can change by various parameter such as voltage, current and etc. Therefore to compare the vibrations, the differential vibration between healthy and faulty condition is used. Using this idea, the part of vibrations that depend on other sources of transformer vibrations, are eliminated. It can be seen that various frequencies are available in vibration signals but the main sources of vibration are forces appearing in the winding and the core. Since vibration depends on current squared and considering that current is practically sinusoidal (50 Hz in This study), the winding vibration main harmonic component is 100 Hz [49-51].

$$F_{\omega} \alpha i^2 \tag{8}$$

It can be seen that with increasing fault severity, the vibration of winding increases and electromagnetic force in radial and axial direction of windings increases too. To verify the calculated electromagnetic forces by FEM, first axial force is calculated by doing simulation if the sensor is placed at the same location and has the same condition as in experimental test, then using curve fitting of MATLAB software, the axial force signal is converted to sinusoidal and cosinusoidal equation. Then these equations are applied to (6) and the vibrations in simulation are calculated. Fig. 16 compares frequency analysis of vibration, for experiment and simulation. It can be seen that at frequency of 100Hz, the error between simulation and experiment is about 5 percent and experimental and simulated calculations are very similar, thus the proper performance of simulations for force calculation is verified.

6 Conclusions

In this paper, transformer interturn short circuit was modelled, and a new method based on vibration analysis is proposed. Electromagnetic forces in axial and radial

directions for various interturn faults in the transformer are investigated, indicating exerted vibrations at fault location. Vibration signature at interturn fault is quite sensitive to the severity of electromagnetic forces, resulting by interturn fault current. According to these conclusions, the transformer vibration monitoring can be used for interturn winding fault detection and online condition monitoring. The results show that faulty windings can be distinguished from normal windings by analyzing the steady-state vibrations. The sensor that used for vibration measurement is very cheap, so this method is very cheap in comparison to other methods for fault detection. This method also can be easily used online for internal fault detection.

References

[1] M. Heathcote, "6 – Operation and maintenance," in *J & P Transformer Book*, 2007, pp. 406–669.

[2] J. Faiz and R. Heydarabadi, "Diagnosing power transformers faults," *Russian Electrical Engineering*, Vol. 85, No. 12, pp. 785–793, Dec. 2014.

[3] I. Metwally, "Failures, Monitoring and New Trends of Power Transformers," *IEEE Potentials*, Vol. 30, No. 3, pp. 36–43, May 2011.

[4] M. Jabloski and E. Napieralska-Juszczak, "Internal faults in power transformers," *IET Electric Power Applications*, Vol. 1, No. 1, p. 105, 2007.

[5] I. Moukhtar, A. Z. El Dein, and O. E. Gouda, "Turn-to-earth fault modelling of power transformer based on symmetrical components," *IET Generation, Transmission & Distribution*, Vol. 7, No. 7, pp. 709–716, Jul. 2013.

[6] H. Wang and K. L. Butler, "Finite element analysis of internal winding faults in distribution transformers," *IEEE Transactions on Power Delivery*, Vol. 16, No. 3, pp. 422–428, Jul. 2001.

[7] P. Bastard, P. Bertrand, and M. Meunier, "A transformer model for winding fault studies," *IEEE Transactions on Power Delivery*, Vol. 9, No. 2, pp. 690–699, Apr. 1994.

[8] Hang Wang and K. L. Butler, "Modeling transformers with internal incipient faults," *IEEE Transactions on Power Delivery*, Vol. 17, No. 2, pp. 500–509, Apr. 2002.

[9] V. Behjat and A. Vahedi, "Numerical modelling of transformers interturn faults and characterising the faulty transformer behaviour under various faults and operating conditions," *IET Electric Power Applications*, Vol. 5, No. 5, pp. 415–431, 2011.

[10] M. S. Ballal, H. M. Suryawanshi, M. K. Mishra, and B. N. Chaudhari, "Interturn faults detection of transformers by diagnosis of neutral current," *IEEE Transactions on Power Delivery*, Vol. 31, No. 3, pp. 1096–1105, Jun. 2016.

[11] A. Abu-Siada and S. Hmood, "A new fuzzy logic approach to identify power transformer criticality using dissolved gas-in-oil analysis," *International Journal of Electrical Power & Energy Systems*, Vol. 67, pp. 401–408, May 2015.

[12] S. S. M. Ghoneim and I. B. M. Taha, "A new approach of DGA interpretation technique for transformer fault diagnosis," *International Journal of Electrical Power & Energy Systems*, Vol. 81, pp. 265–274, Oct. 2016.

[13] H. De Faria, J. G. S. Costa, and J. L. M. Olivas, "A review of monitoring methods for predictive maintenance of electric power transformers based on dissolved gas analysis," *Renewable and Sustainable Energy Reviews*, Vol. 46, pp. 201–209, Jun. 2015.

[14] V. Behjat, A. Vahedi, A. Setayeshmehr, H. Borsi, and E. Gockenbach, "Diagnosing shorted turns on the windings of power transformers based upon online FRA using capacitive and inductive couplings," *IEEE Transactions on Power Delivery*, Vol. 26, No. 4, pp. 2123–2133, Oct. 2011.

[15] V. Behjat and M. Mahvi, "Localising low-level short-circuit faults on the windings of power transformers based on low-frequency response measurement of the transformer windings," *IET Electric Power Applications*, Vol. 9, No. 8, pp. 533–539, Sep. 2015.

[16] S. M. Saleh, S. H. EL-Hoshy, and O. E. Gouda, "Proposed diagnostic methodology using the cross-correlation coefficient factor technique for power transformer fault identification," *IET Electric Power Applications*, Vol. 11, No. 3, pp. 412–422, Mar. 2017.

[17] L. M. R. Oliveira and A. J. M. Cardoso, "Comparing power transformer turn-to-turn faults protection methods: negative sequence component versus space-vector algorithms," *IEEE Transactions on Industry Applications*, Vol. 53, No. 3, pp. 2817–2825, May 2017.

[18] P. A. Venikar, M. S. Ballal, B. S. Umre, and H. M. Suryawanshi, "Sensitive incipient inter-turn fault detection algorithm for power transformers," *IET Electric Power Applications*, Vol. 10, No. 9, pp. 858–868, Nov. 2016.

[19] H. R. Mirzaei, A. Akbari, E. Gockenbach, M. Zanjani, and K. Miralikhani, "A novel method for ultra-high-frequency partial discharge localization in power transformers using the particle swarm optimization algorithm," *IEEE Electrical Insulation Magazine*, Vol. 29, No. 2, pp. 26–39, Mar. 2013.

[20] H. Mirzaei, A. Akbari, E. Gockenbach, and K. Miralikhani, "Advancing new techniques for UHF PD detection and localization in the power transformers in the factory tests," *IEEE Transactions on Dielectrics and Electrical Insulation*, Vol. 22, No. 1, pp. 448–455, Feb. 2015.

[21] P. A. Venikar, M. S. Ballal, B. S. Umre, and H. M. Suryawanshi, "Search coil based online diagnostics of transformer internal faults," *IEEE Transactions on Power Delivery*, Vol. 32, No. 6, pp. 2520–2529, 2017.

[22] M. F. Cabanas, M. G. Melero, F. Pedrayes, C. H. Rojas, G. A. Orcajo, J. M. Cano, and J. G. Iglesias, "A new online method based on leakage flux analysis for the early detection and location of insulating failures in power transformers: Application to remote condition monitoring," *IEEE Transactions on Power Delivery*, Vol. 22, No. 3, pp. 1591–1602, Jul. 2007.

[23] F. Haghjoo and M. Mostafaei, "Flux-based turn-to-turn fault protection for power transformers," *IET Generation, Transmission & Distribution*, Vol. 10, No. 5, pp. 1154–1163, Apr. 2016.

[24] H. Paydarnia, S. Hajiaghasi, and K. Abbaszadeh, "Improved structure of PNN using PCA in transformer fault diagnostic," *Arabian Journal for Science and Engineering*, Vol. 39, No. 6, pp. 4845–4851, Jun. 2014.

[25] A. Wiszniewski, W. Rebizant, and L. Schiel, "New algorithms for power transformer inter-turn fault protection," *Electric Power Systems Research*, Vol. 79, No. 10, pp. 1454–1461, Oct. 2009.

[26] N. Asadi and H. M. Kelk, "Modeling, analysis, and detection of internal winding faults in power transformers," *IEEE Transactions on Power Delivery*, Vol. 30, No. 6, pp. 2419–2426, Dec. 2015.

[27] A. S. Masoum, N. Hashemnia, A. Abu-Siada, M. A. S. Masoum, and S. M. Islam, "Online transformer internal fault detection based on instantaneous voltage and current measurements considering impact of harmonics," *IEEE Transactions on Power Delivery*, Vol. 32, No. 2, pp. 587–598, Apr. 2017.

[28] H. Balaga, N. Gupta, and D. N. Vishwakarma, "GA trained parallel hidden layered ANN based differential protection of three phase power transformer," *International Journal of Electrical Power & Energy Systems*, Vol. 67, pp. 286–297, May 2015.

[29] H. Dashti and M. Sanaye-Pasand, "Power transformer protection using a multiregion adaptive differential relay," *IEEE Transactions on Power Delivery*, Vol. 29, No. 2, pp. 777–785, Apr. 2014.

[30] L. Sevov, U. Khan, and Z. Zhang, "Enhancing power transformer differential protection to improve security and dependability," *IEEE Transactions on Industry Applications*, Vol. 53, No. 3, pp. 2642–2649, May 2017.

[31] M. H. Wang, "Extension neural network for power transformer incipient fault diagnosis," *IEE Proceedings - Generation, Transmission and Distribution*, Vol. 150, No. 6, pp. 679-685, 2003.

[32] S. Bagheri, Z. Moravej, and G. B. Gharehpetian, "Classification and discrimination among winding mechanical defects, internal and external electrical faults and inrush current of transformer," *IEEE Transactions on Industrial Informatics*, Vol. 14, No. 2, pp. 484–493, 2018.

[33] M. Rahmatian, B. Vahidi, A. J. Ghanizadeh, G. B. Gharehpetian, and H. A. Alehosseini, "Insulation failure detection in transformer winding using cross-correlation technique with ANN and k-NN regression method during impulse test," *International Journal of Electrical Power & Energy Systems*, Vol. 53, No. 1, pp. 209–218, Dec. 2013.

[34] H. Malik, A. K. Yadav, S. Mishra, and T. Mehto, "Application of neuro-fuzzy scheme to investigate the winding insulation paper deterioration in oil-immersed power transformer," *International Journal of Electrical Power & Energy Systems*, Vol. 53, No. 1, pp. 256–271, Dec. 2013.

[35] H. Zhou, K. Hong, H. Huang, and J. Zhou, "Transformer winding fault detection by vibration analysis methods," *Applied Acoustics*, Vol. 114, pp. 136–146, Dec. 2016.

[36] M. Bagheri and B. T. Phung, "Frequency response and vibration analysis in transformer winding turn-to-turn fault recognition," in *2016 International Conference on Smart Green Technology in Electrical and Information Systems (ICSGTEIS)*, pp. 10–15, 2016.

[37] H. M. Ahn, Y. H. Oh, J. K. Kim, J. S. Song, and S. C. Hahn, "Experimental verification and finite element analysis of short-circuit electromagnetic force for dry-type transformer," *IEEE Transactions on Magnetics*, Vol. 48, No. 2, pp. 819–822, Feb. 2012.

[38] J. F. Araujo, E. G. Costa, F. L. M. Andrade, A. D. Germano, and T. V. Ferreira, "Methodology to evaluate the electromechanical effects of electromagnetic forces on conductive materials in transformer windings using the von mises and fatigue criteria," *IEEE Transactions on Power Delivery*, Vol. 31, No. 5, pp. 2206–2214, Oct. 2016.

[39] A. Najafi and I. Iskender, "Electromagnetic force investigation on distribution transformer under unbalanced faults based on time stepping finite element methods," *International Journal of Electrical Power & Energy Systems*, Vol. 76, pp. 147–155, Mar. 2016.

[40] M. Patel, "Dynamic response of power transformers under axial short circuit forces PART I - Winding and clamp as individual components," *IEEE Transactions on Power Systems*, Vol. PAS-92, No. 5, pp. 1558–1566, Sep. 1973.

[41] M. Patel, "Dynamic response of power transformers under axial short circuit forces Part II - Windings and clamps as a combined system," *IEEE Transactions on Power Apparatus and Systems*, Vol. PAS-92, No. 5, pp. 1567–1576, Sep. 1973.

[42] Y. Hori and K. Okuyama, "Axial vibration analysis of transformer windings under short circuit conditions," *IEEE Transactions on Power Apparatus and Systems*, Vol. PAS-99, No. 2, pp. 443–451, Mar. 1980.

[43] Q. Li, X. Wang, L. Zhang, J. Lou, and L. Zou, "Modelling methodology for transformer core vibrations based on the magnetostrictive properties," *IET Electric Power Applications*, Vol. 6, No. 9, pp. 604–610, 2012.

[44] Y. Yang, L. Qingfen, L. Dichen, L. Shanshan, and H. Jingzhu, "Electromagnetic vibration noise analysis of transformer windings and core," *IET Electric Power Applications*, Vol. 10, No. 4, pp. 251–257, Apr. 2016.

[45] Y. Wang and J. Pan, "Comparison of mechanically and electrically excited vibration frequency responses of a small distribution transformer," *IEEE Transactions on Power Delivery*, Vol. 32, No. 3, pp. 1173–1180, Jun. 2017.

[46] E. Rivas, J. C. Burgos, and J. C. Garcia-Prada, "Vibration analysis using envelope wavelet for detecting faults in the OLTC tap selector," *IEEE Transactions on Power Delivery*, Vol. 25, No. 3, pp. 1629–1636, Jul. 2010.

[47] G. B. Kumbhar and S. V. Kulkarni, "Analysis of short-circuit performance of split-winding transformer using coupled field-circuit approach," *IEEE Transactions on Power Delivery*, Vol. 22, No. 2, pp. 936–943, Apr. 2007.

[48] H. M. Ahn, J. Y. Lee, J. K. Kim, Y. H. Oh, S. Y. Jung, and S. C. Hahn, "Finite-element analysis of short-circuit electromagnetic force in power transformer," *IEEE Transactions on Industry Applications*, Vol. 47, No. 3, pp. 1267–1272, May 2011.

[49] B. Garcia, J. C. Burgos, and A. M. Alonso, "Transformer tank vibration modeling as a method of detecting winding deformations—Part II: Experimental verification," *IEEE Transactions on Power Delivery*, Vol. 21, No. 1, pp. 164–169, Jan. 2006.

[50] B. Garcia, J. C. Burgos, and A. Alonso, "Transformer tank vibration modeling as a method of detecting winding deformations—Part I: Theoretical foundation," *IEEE Transactions on Power Delivery*, Vol. 21, No. 1, pp. 157–163, Jan. 2006.

[51] S. Hajiaghasi, A. Salemnia, and F. Motabarian, "Transformer condition monitoring for internal fault detection based on vibration frequency response analysis" in *Power Systems Protection & Control Conference*, Jan. 2016.

S. Hajiaghasi was born in Qazvin, Iran, in 1987. He is currently Ph.D. student of Electrical Engineering at Shahid Beheshti University (SBU), Tehran, Iran. His research interests include power electronic, electrical machines, renewable energy, and microgrids.

K. Abbaszadeh received the B.Sc. degree in Communication Engineering from Khajeh Nasir Toosi University of Technology, Tehran, Iran, in 1991, and the M.Sc. and Ph.D. degrees in Electrical Engineering from Amir Kabir University of Technology, Tehran, Iran, in 1997 and 2000, respectively. From 2001 to 2003, he was a Research Assistant with the Department of Electrical Engineering, Texas A&M University, College Station, TX, USA. He is currently Professor with the Department of Electrical Engineering, Khajeh Nasir Toosi University of Technology. His research interests include power electronic and DC–DC and DC–AC converters, electric machinery, variable-speed drives, and propulsion applications.

A. Salemnia received the B.Sc. and M.Sc. degrees from Iran University of Science and Technology (IUST), Tehran, Iran, in 1983 and 1990, respectively, and the Ph.D. degree from Polytechnic Institute of Lorraine (INPL), France, in 1996, all in Electrical Engineering. He joined Shahid Beheshti University (SBU), Tehran, Iran, in 1990, where he is currently an Assistant Professor. His research interests include power quality, harmonics and active filtering.